DOI 10.1364/OE.27.021622
ISSN 1094-4087

Publisher: Optica

European Regional Development Fund (CZ.02.1.01/0.0/0.0/15_006/0000674); Horizon 2020 research and innovation programme (739573); Ministry of Education, Youth and Sports of the Czech Republic (LO1602, LM2015086).

Research Article | Vol. 27, No. 15 | 22 Jul 2019 | OPTICS EXPRESS 21622
Optics EXPRESS

Novel unstable resonator configuration for highly efficient cryogenically cooled Yb:YAG Q-switched laser

JÖRG KÖRNER,[1,2,*] SANIN ZULIĆ,[1] DANIJELA ROSTOHAR,[1] ANTONIO LUCIANETTI,[1] AND TOMÁŠ MOCEK[1]

[1] *HiLASE Centre, Institute of Physics of the Czech Academy of Sciences, Za Radnicí 828, 252 41 Dolní Břežany, Czech Republic*
[2] *Institute of Optics and Quantum Electronics, Friedrich-Schiller University, Max-Wien Platz 1, 07743 Jena, Germany*
[*] *joerg.koerner@uni-jena.de*

Abstract: A novel method to shape the intensity distribution within an unstable laser cavity is demonstrated. This method is characterized by inscribing a tailored gain profile generated by a spatially tophat-shaped longitudinal pump beam into the gain medium. The mode shaping mechanism is still effective with zero output coupling. Therefore, this method enables to operate unstable laser cavities in cavity dump mode or as a regenerative amplifier. The theoretical background is described by means of geometrical optics, and operation of a prototype setup using cryogenically cooled Yb:YAG is demonstrated. The system produces 13 ns pulses with 285 mJ at a repetition rate of 10 Hz, with an extraction efficiency of 35 %. Successful cavity dump operation is demonstrated with 110 mJ output energy.

1. Introduction

Reliable and compact high-energy-class solid state lasers that can deliver multi Joule nanosecond pulses have attracted increasing interest in recent years. These lasers are used not only in fundamental science as pump sources for petawatt class Titanium sapphire laser systems (e.g. [1]), but also for high impact industrial applications like laser shock peening and advanced material treatments [2].

Today industrial lasers of this category are mostly based on Nd^{3+} doped laser media. While for systems with high pulse energy flash-lamp pumped Nd:glass is typically chosen, laser systems with the need for high repetition rates rely on laser diodes as pump source in combination with Nd:YAG or Nd:YLF. As a result of this, the efficiency is significantly increased and the thermal load, which is limiting the average output power, is drastically reduced.

In this context, the main drawbacks of using Nd^{3+}- doped gain media is the relatively short fluorescence lifetime, which increases the minimum laser diode pump power to store a specific amount of energy in the laser medium. Furthermore, the relatively high quantum defect around 25 % still leads to significant heat generation.

In comparison, Yb^{3+} doped media offer about four times longer fluorescence lifetime and 2.5 times lower quantum defect. Accordingly, the diode power needed in pulsed operation can be much lower and such laser materials can operate with significantly higher average powers. However, the performance using these active media is limited due to the re-absorption induced by the low separation of pump and laser wavelength. A great effort has been spent to overcome this issue. The most common approach is to use cryogenic cooling, which cancels the re-absorption, increases the peak cross sections, and improves the thermo-mechanical properties of most laser materials [3,4]. This allows laser systems to be operated at high average powers in the kW range (e.g. [5,6]) as well as to reach a record efficiency of more than 45 % of optical to optical efficiency

#362029 https://doi.org/10.1364/OE.27.021622
Journal © 2019 Received 21 Mar 2019; revised 14 Jun 2019; accepted 17 Jun 2019; published 17 Jul 2019

for a Joule class nanosecond laser amplifier based on cryogenic cooled Yb:YAG in pulse pumped mode [7].

Recently, further scaling in energy and repetition rate has been demonstrated with scientific large scale laser systems achieving more than 100 J at a repetition rate of 10 Hz [8].

However, such large scale systems are very complex and typically consist of a chain of individual amplifiers starting at the sub milli-Joule level. Hence, the application of these lasers in industrial environments is strongly limited. A major step with the goal to simplify such systems must be taken to broaden the field of applications.

Reducing the number of amplifiers or even completely switching to direct generation of J-level laser pulses is a major task for future developments. In case of Nd^{3+}-doped media, such high energy nanosecond oscillators are realized with a Q-switched unstable cavity. This approach allows direct generation of large mode size beams with excellent beam quality. Furthermore, since graded reflectivity mirrors (GRM) are state of the art since the early nineties [9], the output beam profile can be properly chosen to resemble a super Gaussian intensity distribution. This is convenient for further amplification with a master oscillator power amplifier scheme.

The major drawback of this approach is that, due to the characteristics of a GRM, the feedback generated in such laser cavity is relatively low [10], and therefore not compatible with low gain media like most Yb^{3+}-doped materials.

In this work, we present an alternative approach for generating a well defined intra- and extra-cavity intensity distribution within an unstable cavity. Instead of a loss based shaping mechanism, we use a tailored gain distribution inscribed by a co-propagating spatially-shaped pump beam. This is realized by a homogenized laser diode pump module as is commonly used in many high energy Yb^{3+}-based laser systems.

Using this approach, we have demonstrated the possibility of using a significantly higher feedback than in GRM designs, while maintaining a flattop intensity distribution. This enables the use of laser media with lower gain. Furthermore, such layout is operable even without output coupling, while still generating a flat top intensity distribution inside the cavity. This allows operation in cavity dumped mode or as regenerative amplifier, and greatly extends the potential use of unstable cavities in general. This approach was filed for our patent in Czech republic under the filing number PV 2018-228.

In this paper, we also present the results from the operation of a prototype laser based on the described principle. A cryogenically cooled Yb:YAG crystal was used as the active medium. The prototype achieved an output energy of 280 mJ at 10 Hz with a pulse length of about 13 ns. The output profile was a rectangular tophat beam very much resembling the profile of the used pump module. Furthermore, we report about the laser operation with different output coupling and in cavity dump mode.

2. Theoretical background

Unstable laser cavities were proposed since the invention of the first lasers [11]. We use the geometrical optic description from [10] to explain the basic principle behind our approach, which we refer to as gain-modulation.

Following this reference, a resonator in paraxial approximation can be described by the ABCD matrix for one round-trip in the cavity. In an unstable cavity, the wavefront radius of curvature of the generated beam must be maintained throughout the cavity round-trips. Hence, the criterion to be fulfilled in an unstable laser cavity is:

$$|G| := \frac{|A + B|}{2} \geq 1 \tag{1}$$

Here, A and B are the according matrix elements. Another important parameter that will be used

Optics EXPRESS

to describe an unstable cavity is the magnification per round-trip in the cavity M:

$$M = G + \frac{|G|}{G} \cdot \sqrt{G^2 - 1} \tag{2}$$

A major development in the field of unstable laser cavities was the implementation of so called Gaussian reflectivity mirrors (GRM) in the late eighties (cf. e.g. [12]). Such a mirror features a radially symmetric reflectivity profile $R(r)$ with a super Gaussian distribution as a function of the distance to the optical axis r:

$$R(r) = R_0 \cdot e^{-2 \cdot \left(\frac{r}{\omega_{GRM}}\right)^{GO}} \tag{3}$$

Here ω_{GRM} is the $^1/_{e^2}$ width of the reflectivity distribution, GO the super Gaussian order of the reflectivity profile, and $r = \sqrt{x^2 + y^2}$ the distance from the optical axis. The highest reflectivity R_0 is in the center of the mirror, while the reflectivity fades out with increasing distance r from the optical axis. Such an output coupler allows to generate a smooth tophat output beam profile, without sharp apertures causing fringing patterns on the beam profile.

Such a mirror can be included in the geometrical optical modelling of a cavity, which allows to determine the intra-cavity intensity $I_{cav}(r)$ profile using:

$$I_{cav}(r) = I_0 \cdot \prod_{k=1}^{\infty} \left(\frac{R(\frac{r}{M^k})}{R_0} \right) \tag{4}$$

Here I_0 is the intensity in the middle of the beam.

By combining Eqs. 3 and 4, the intra-cavity intensity distribution is obtained:

$$I_{cav}(r) = I_0 \cdot e^{-2 \cdot \left(\frac{r}{\omega_{GRM} \cdot (M^{GO} - 1)^{1/GO}} \right)^{GO}} \tag{5}$$

From Eq. 5 it can be seen that the intra-cavity intensity distribution resembles a tophat shaped profile of the same super-Gaussian order as the GRM's reflectivity profile with a slightly enlarged radius. The output intensity profile I_{out} is obtained by multiplying Eq. 5 with the transmission of the GRM $T(r) = 1 - R(r)$:

$$I_{out}(r) = I_{cav}(r) \cdot (1 - R(r)) \tag{6}$$

Contrary to the intra-cavity beam profile, the output beam can feature a lower intensity in its central area when the reflectivity in the center of the GRM is too high. This leads to a so called "flat-top condition", determining the maximum reflectivity in the center of the output coupler, for which no intensity drop in the beam center is observed. It is obtained by setting the second derivation of Eq. 6 equal to zero:

$$R_0 \leq \frac{1}{M^{GO}} \tag{7}$$

Due to stability considerations, the magnification of an unstable cavity cannot be made infinitely small. Hence, the usage of such GRM unstable cavity design is limited to high gain laser media, which can balance the low feedback linked with the maximum reflectivity of the GRM with sufficient amplification. This holds especially true if steeper edges of the intensity profile, and therefore a higher Gaussian order, is desired. This is especially desirable to optimize the spatial overlap of the pumped laser material's aperture with the intra-cavity intensity distribution.

In the approach presented in this work, we propose to use a spatially tailored gain profile instead of a GRM. Hereby, the basic working principle is similar to a GRM design, but instead of introducing additional losses at the edges of the beam to limit its spatial extension, a spatially confined gain area introduces a gain-modulation in the beam's center.

Optics EXPRESS

The maximum double pass gain G_0^2 in the center of the beam is selected to balance the intensity losses per round-trip due to the reflectivity of the output coupler and the magnification:

$$G_0^2 = \frac{M^2}{R_0} \tag{8}$$

Furthermore, we will assume a super-Gaussian double pass gain $G(r)^2$ distribution in analogy to the profile of the previously described GRM with an offset of 1, denoting that there are no losses outside the pumped region:

$$G(r)^2 = (G_0^2 - 1) \cdot e^{-2\cdot\left(\frac{r}{\omega_g}\right)^{GO}} + 1 \tag{9}$$

Here, ω_g is the $1/e^2$ width of the double pass gain distribution. The intra-cavity intensity distribution can be calculated numerically using a sufficient number of terms of the product series:

$$I_{cav}(r) = I_0 \cdot \prod_{k=0}^{\infty} \frac{G(\frac{r}{M^k})^2}{G_0^2} \tag{10}$$

Here, $k = 0$ is needed to include an amplification at the end of the last round-trip. The corresponding output beam profile will have the same intensity distribution as I_{cav} as the output coupling is independent on space.

In the following, we will consider the resulting intensity distribution using the first factors of Eq. 10:

$$\begin{aligned} I_{cav} = I_0 \cdot & \left[\left(1 - \frac{1}{G_0^2}\right) \cdot e^{-2\cdot\left(\frac{r}{\omega_g M}\right)^{GO}} + \frac{1}{G_0^2} \right] \\ & \cdot \left[\left(1 - \frac{1}{G_0^2}\right) \cdot e^{-2\cdot\left(\frac{r}{\omega_g M^2}\right)^{GO}} + \frac{1}{G_0^2} \right] \\ & \cdot \left[\left(1 - \frac{1}{G_0^2}\right) \cdot e^{-2\cdot\left(\frac{r}{\omega_g M^3}\right)^{GO}} + \frac{1}{G_0^2} \right] \cdot \ldots \end{aligned} \tag{11}$$

Again, this can be transformed into a sum of products by performing the multiplications. Assuming a reasonably steep edge of the gain distribution, the spatial shape from each of these summands is defined by the lowest k exponential term contained in the product. In this case the central area will be dominated by a flattop profile that resembles the according exponential term, while all higher k terms will not significantly contribute. This is because all higher order terms are flattop profiles with a greater diameter, which will be spatially tailored by the lower k term and thus do not add additional structure inside the flat top area. In this case, these terms can be approximated with 1. This leads to an overall approximation for the beam profile:

$$I_{cav} \approx I_0 \cdot \sum_{k=0}^{\infty} \left(1 - \frac{1}{G_0^2}\right) \cdot e^{-2\cdot\left(\frac{r}{\omega_g M^{k+1}}\right)^{GO}} \cdot \frac{1}{G_0^{2k}} \tag{12}$$

The resulting profile will resemble a step pyramid, where each step is broader than the last step by a factor of M and has an intensity, which is $1/G_0^{2n}$ times the intensity of the beams center. Here $n = 0$ assigns the top of the pyramid and is counted from top to bottom on point of intensity.

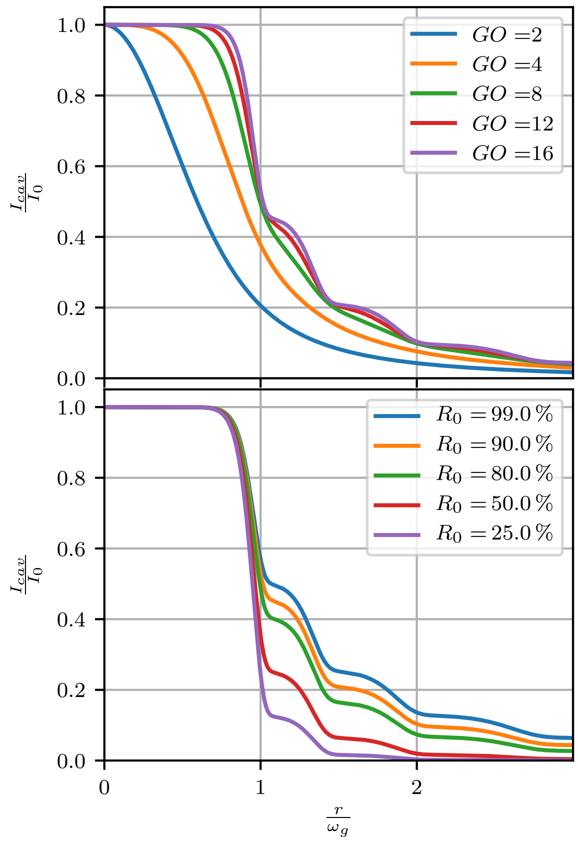

Fig. 1. Cross sections of the intra-cavity intensity distribution I_{cav}. The simulated cavity has a magnification of $M = 1.4$. The gain G_0^2 is adjusted according to Eq. 8. Upper graphs: The reflectivity of the output mirror is kept constant at $R_0 = 90\%$, while the Gaussian order of the gain distribution GO is varied. Lower graphs: $GO = 16$ is kept constant, while the output coupler's reflectivity R_0 is varied.

A simple simulation based on a numerical calculation of Eq. 10 with varying input parameters is shown in Fig. 1.

The relative intensity of the steps can be suppressed in several ways. In case of a high gain amplifier, like in most q-switch amplifiers, the intensity of the steps will be relatively low as $1/G_0^2 \ll 1$ (cf. Fig. 1 lower graph). According to Eq. 8, this requires either a large value of M or high output coupling. Furthermore, for reduced edge steepness of the gain profile and low magnification, the steps will be smeared out in the edges of the beam profile (cf. Fig. 1 upper graph).

Contrary to GRM layouts, a flattop condition does not exist. Therefore, the output coupling can be even completely omitted, without losing the principal intra-cavity beam shaping mechanism. Furthermore, as the reflectivity of the output coupler is spatially uniform, it can be convenient to use a variable output coupler e.g. realized by a polarizer in combination with a wave-plate. Combining this kind of output coupling with an electro-optical switch enables to use an unstable cavity in a cavity dump operation mode or as regenerative amplifier. To the best of our knowledge, this has never been realized with unstable cavity layouts so far. The cavity dump operation is also demonstrated with the test system described in this work.

Another interesting aspect of this type of layout is that the shaping mechanism will work for all shapes of tophat beams, as long as the intensity is monotonously decreasing from the center to its edges. This especially covers shapes that are nowadays common for homogenized laser diode pump beams like round, rectangular or hexagonal and therefore allows for flexibility with respect to the output beam profile. A simulation of output beam profiles with various gain distributions are shown in Fig. 2 with varying parameters. The simulation is based on Eq. 10 with a magnification of $M = 1.4$.

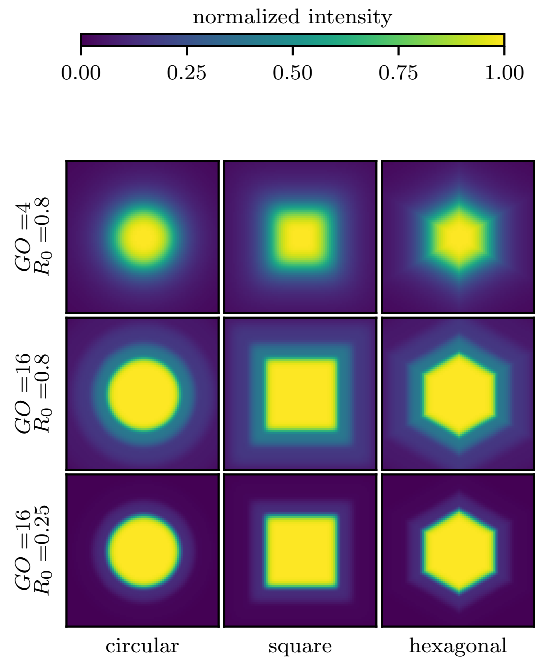

Fig. 2. Simulated output intensity profiles for differently shaped gain distributions. From left to right: circular, square, hexagonal. From top to bottom: different combinations of Gaussian order of the gain profile GO and the reflectivity of the output coupler R_0 as indicated on the left side. The cavity magnification was fixed at $M = 1.4$. The gain G_0^2 is adjusted according to Eq. 8.

With respect to the extraction efficiency, it can be stated that this kind of cavity layout offers the potential for highly efficient lasers, as an overlap of pumped area and intra-cavity intensity distribution is automatically established and no clipping apertures reduce the efficiency.

Finally, it should be mentioned that for a more detailed analysis of a given cavity, a model taking into account the diffraction of the beam during propagation should be used. Such methods are well described in the literature (cf. e.g. [10]) and can also be adapted in the technique described here.

3. Setup

In order to test our theoretical predictions, we realized a laser setup based on a cryogenically cooled Yb:YAG crystal gain medium (28 mm diameter, 4.5 mm thick, 3at.% doped). As the focus of this work is related to the proof of principle of the gain-modulated unstable cavity approach, we refrained from using a specialized high performance cooling scheme. Hence, the crystal was thermally contacted to a copper heat sink by clamping the crystal in a ring shaped area of an

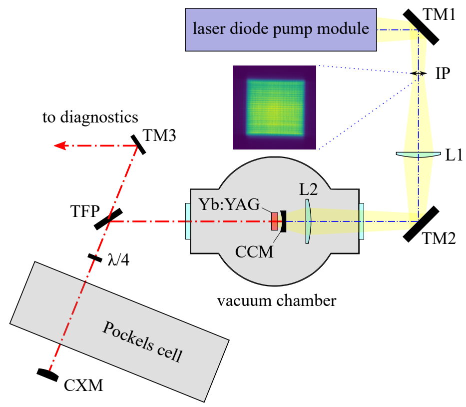

Fig. 3. Schematic setup of the laser system. It is: CCM: concave mirror with radius of 4 m, CXM: convex mirror with radius of 5 m, IP: intermediate image plane of the homogenized pump beam, L1 and L2: lenses, $\lambda/4$: quarter wave plate, TFP: thin film polarizer, TM1 to TM3 turning mirrors.

approximate width of 4 mm close to the crystals edge on both surfaces using indium foil for thermal contact. The crystal's mount itself was directly connected to the cold finger of a liquid nitrogen bath cryostat. The vacuum chamber of the cryostat was held under high vacuum in the range of 10^{-7} mbar to 10^{-6} mbar to ensure the thermal insulation and avoid condensation on the crystal's surface.

The 0.5m long laser cavity was formed by two mirrors, a convex mirror with a radius of 4 m (CXM) and a concave mirror with a radius of 5 m (CCM), as shown in Fig. 3. The latter mirror was placed inside the cryostat close to the laser crystal and was coated with a dichroic coating being highly reflective at the laser wavelength of 1030 nm and low reflective at the pump wavelength at 940 nm. This allows efficient coupling of the pump beam with the laser mode into the laser material.

An homogenized laser diode module (PM2.4, Lastronics GmbH) was used as pump source, delivering up to 1.69 kW in a square shaped tophat beam profile in an external image plane (IP, cf. inset in Fig. 3) that was re-imaged into the crystal to a size of 4.5 mm by 4.5 mm with a telescope (L1 and L2). The pump wavelength corresponded to the 940 nm absorption band of Yb:YAG and was fine adjusted to the absorption maximum by varying the cooling water temperature.

Output coupling was realized by folding the cavity with a 56° thin film polarizer (TFP) in combination with a quarter wave plate ($\lambda/4$), allowing for adjustable output coupling in dependence of its rotation. Additionally, q-switch and cavity dump operation of the cavity was realized with a KD*P Pockels cell (impact 13, Gooch & Housego PLC) inserted into the cavity. The cell was operated using a push-pull high voltage switch (Bergmann Messgeräte Entwicklung KG).

To measure the output beam profile a reflection from a wedged plate was imaged onto a CCD camera (Manta G-125B PoE, Allied Vision Technologies GmbH). The imaging setup was designed to reproduce an image of the crystal plane within the amplifier to minimize propagation effects.

4. Results

First tests of the laser cavity were performed without the Pockels cell installed in the cavity under quasi continuous wave (QCW) operation. The pump diodes were operated at maximum current generating an output peak power of 1.69 kW and with a pulse duration of 850 µs at

10 Hz repetition rate. Output pulse energy and beam profile as a function of the internal quarter waveplate's rotation angle were recorded. The results are illustrated in Fig. 4. A wave plate angle of 282° corresponds to minimum output coupling.

From the corresponding profiles, it can be seen that the output profile is well defined for high output coupling, while for higher cavity feedback additional parts of the beam outside the central tophat area are appearing. Even though these are partly clipped in our setup, this corresponds well with the predictions from the theoretical description. The output profile corresponds well with the pump profile (cf. inset in Fig. 3), though it has a slightly rectangular shape and exhibits stronger intensity modulations. The latter one was attributed to relatively low quality of the laser crystal used in combination with residual modulations in the pump beam. The rectangular shape originates from the asymmetric opening angle of the pump beam, which shows stronger divergence in the horizontal axis corresponding to the diodes slow axis. Therefore, the accumulated gain profile in the crystal does not exactly resemble a square, but rather a rectangle shape due to the propagation effects of the pump beam.

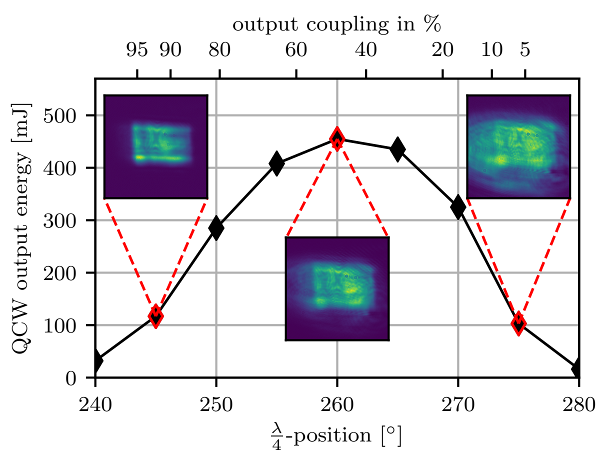

Fig. 4. Output energy of the laser cavity in QCW operation. Pump parameters were 1.69 kW, 850 µs and 10 Hz repetition rate. The output beam profiles in the insets correspond to the marked measurement points.

The Pockels cell was inserted into the cavity for Q-switched operation . The quarter wave plate was adjusted to maximum output coupling blocking laser operation while the Pockels cell was turned off. The Pockels cell was switched on at the end of the pump pulse. The pump diodes were operated with 1.69 kW peak power and repetition rate of 10 Hz. The output pulse energy was measured in dependence of the pump pulse duration, while the Pockels cells' voltage and herewith the output coupling was adjusted to achieve the maximum output energy. The results from this measurement are shown in Fig. 5. The output energy is increasing nearly linear with the pump pulse duration for values up to about 500 µs. The output energy of about 280 mJ remains nearly constant for pump pulse durations of more than 800 µs . As the excited state lifetime for Yb:YAG is known to be in the range of 950 µs [3, 13], a significant increase of the stored energy and therefore the output energy should be observed for up to approximately two times the used pump duration. This indicates that the energy storage is limited in the current setup by amplified spontaneous emission (ASE) in transverse direction. This behavior was to be expected because the Yb:YAG crystal we used was not surrounded by an absorber like cladding.

To estimate the extraction efficiency, we measured the transmitted pump energy at full power, resulting in an absorption of 69%. The extraction efficiency was then determined as the fraction

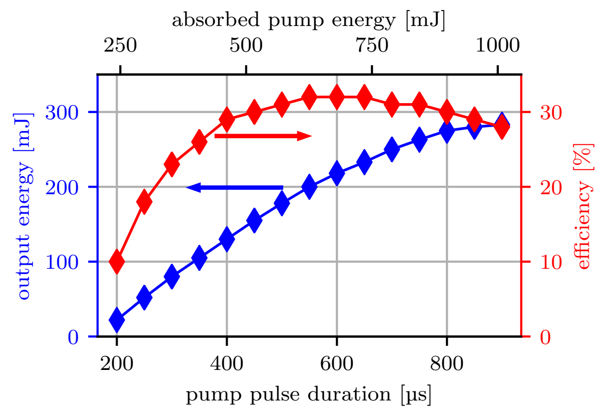

Fig. 5. Output energy (blue) and efficiency (red) as a function of the pump pulse duration.

of the output energy and the absorbed pump energy as a function of the pump pulse duration (cf. Fig. 5). Even if we ignore sources of loss for the pump beam (e.g. approx. 10% of the pump energy were in ghosts images, losses in pump beam transportation optics), the maximum efficiency is 32% from absorbed pump energy to output pulse energy. The output pulse duration was measured using a photo detector (DET10-A, Thorlabs inc.). At maximum output energy the pulse duration was 13±1 ns with a standard q-switch pulse shape. For lower output energy of 200 mJ and 100 mJ the pulse duration was 20 ns and 30 ns, respectively.

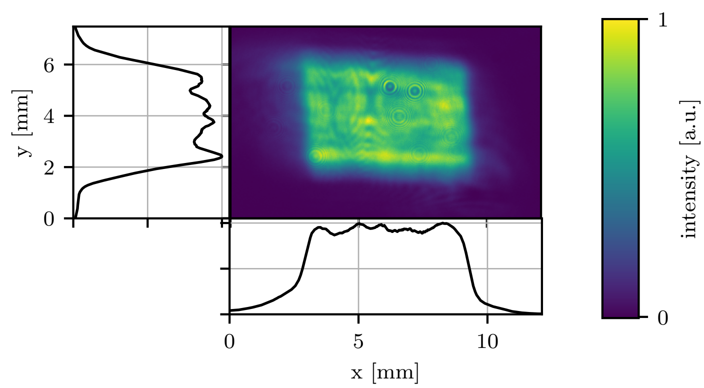

Fig. 6. Output laser profile for q-switch operation. The black curves at the sides are the integrated cross sections.

The output laser profile at 285 mJ output energy is shown in Fig. 6 and an according wavefront measurement in Fig. 7. The rectangular output profile shows good resemblance with the pump profile. The modulations on the intensity plateau are slightly reduced compared to QCW operation, which could be attributed to a slightly improved alignment, using a shifted position in the laser crystal. The phase front shows no severe deformation and indicates a high beam quality.

To test long term stability of the system, we operated the system at 850 µs pump duration in q-switch mode over several hours. The output energy was recorded for every shot (cf. Fig. 8). After initial warm up and a slight realignment at about 55 min after start, the system operated over 2.5 h with an energy standard deviation of 0.72%. After this period, we stopped refilling

Optics EXPRESS

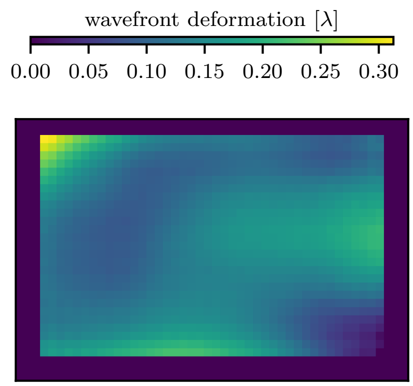

Fig. 7. Phase front measurement of the output beam after removal of tilt and defocus.

liquid nitrogen to the cryostat, leading to a slow warm up of the crystal, while the laser was kept running to test the sensitivity with respect to temperature change. In the beginning, a slight increase in the output energy was observed. This is either attributed to a reduction in ASE or a higher absorption of the pump beam due to an improved spectral overlap caused by broadening of the spectral absorption peaks [3]. With further increase of the temperature, the output energy slowly decreased, which is linked to the reduced cross sections at pump and laser wavelengths. Nevertheless, the laser was operable over a wide temperature range of more than 100 K, while the output energy was reduced by only about 30%, though the pulse length was significantly increased to 30 ns at the end of the experiment, due to the reduced emission cross sections. To maintain maximum output energy, the Pockels cell voltage was constantly optimized during the temperature change. In principle, the laser was still operable even above -100°C when we switched off the system, but we refrained from going to higher temperatures, as the energy and pulse parameters were worse compared to cryogenic operation.

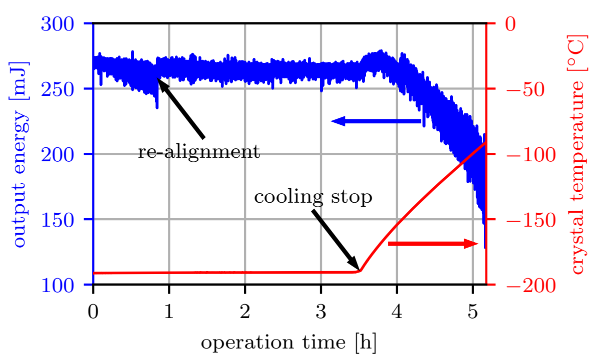

Fig. 8. Energy (blue) and temperature(red) readings over a period of several hours. Cooling was stopped at 3.5 h.

As mentioned in the theoretical background, a major difference to prior concepts for unstable cavities, our approach allows to operate such cavity with zero output coupling. Hence, besides widely used q-switch operation, the laser can easily operate in cavity dump regime. For this purpose, the Pockels cell is tuned to exactly counter the quarter wave plate in the cavity when

Optics EXPRESS

switched on at the end of the pump pulse. Then the intra-cavity intensity is increasing until the residual cavity losses, e.g. the magnification, balance the saturating gain. After this the intra-cavity intensity is decreasing. The Pockels cell is typically switched off at maximum intra-cavity intensity, so a pulse with a length matching one round-trip in the cavity is extracted. This allows to generate a shorter pulse length as in q-switch mode that is independent on the gain.

To verify the possibility of this operation scheme, we tuned the Pockels cell voltage accordingly. To avoid the risk of laser induced damage, the cavity dump experiment was carried out with a reduced peak power of about 760 W from the laser diode pump engine. The pump duration was kept at 850 µs. The resulting output energy as a function of the delay between on and off switching of the Pockels cell is shown in Fig. 9. The insets show the output beam profile at the according delay. The maximum output energy of 110 mJ was achieved for a delay of 105 ns. Taking into account an absorbed pump energy of 450 mJ, this corresponds to an extraction efficiency of roughly 24.5%. With respect to the reduced pump power this indicates a similar performance as in q-switched operation. The obtained output pulse length was 6.2 ns, which is slightly longer than the round-trip time of 3.3 ns. This longer pulse duration is due to the limited rise and fall time of the Pockels cells.

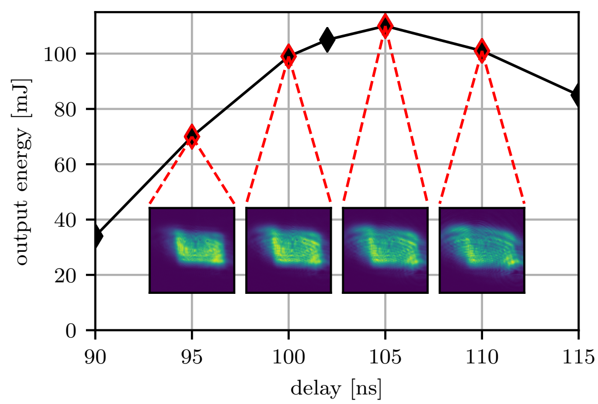

Fig. 9. Output energy as a function of the Pockels cells' delay time in cavity dump operation. The diode current was reduced to 150 A yielding an absorbed pump energy of approximately 450 mJ. The inset beam profiles correspond to the according measurement points as marked by the red dotted lines.

From the recorded output beam profiles, it can be noticed that the exact time for extracting the pulse from the cavity is crucial. For early extraction before maximum intra-cavity intensity the beam profile is well defined with sharp edges. As the gain saturates, the beam profile edges become washed out. This effect again corresponds well with the theoretical description as the discrimination of the intensity steps is reduced due to the gain saturation (cf. Fig. 1 lower graph, where lower gain corresponds to larger R_0).

5. Conclusion

In this work, we have described a novel scheme for shaping the intra- and extra-cavity intensity distribution in an unstable laser resonator. This is obtained by inscribing a spatially tailored flattop gain profile into the active medium, which can be conveniently generated by a homogenized laser diode pump engine in an end pumped configuration. By calculating the resulting laser intensity distribution, we demonstrated that in contrast to GRM based layouts a flattop output intensity distribution is generated independently from the cavity output coupling. This approach enables a higher feedback in the cavity, and also operation of unstable cavities without output coupling at all. Therefore, to the best of our knowledge, this is the first time that unstable laser cavities can potentially be used for operation in cavity dump mode or for regenerative amplification. It was also demonstrated that the laser intensity distribution will very much follow the shape of the pump profile, which allows a high degree of flexibility with respect to the shape of the output profile.

The proposed scheme was verified with a prototype cavity based on cryogenically cooled Yb:YAG. In Q-switched operation, 285 mJ at 10 Hz repetition were obtained with a rectangular beam profile. The efficiency from the absorbed pump energy to laser output energy was about 35 %, which is significantly higher than the efficiency obtained in typical multi-pass high energy amplifiers based on cryogenic Yb:YAG (e.g. [14]). Operation in cavity dump mode was successfully demonstrated with a maximum output energy of 110 mJ and pulse duration of 6.2 ns. These results demonstrate that the use of a homogenized longitudinal laser diode pump in combination with an unstable resonator is a powerful approach to realize compact high-energy Q-switched Yb:YAG lasers.

It is important to note that by optimizing the prototype's setup, the proposed concept will enable to achieve even higher efficiency and output energy. As the major limitation in point of output energy is caused by ASE and transverse lasing, a major step to increase the performance would be to replace the laser medium with a medium with according ASE countermeasures like a cromium absorber cladding. With such adaptions this concept has great potential to trigger a new generation of highly efficient, compact, high-energy class lasers for various applications.

Funding

European Regional Development Fund (CZ.02.1.01/0.0/0.0/15_006/0000674); Horizon 2020 research and innovation programme (739573); Ministry of Education, Youth and Sports of the Czech Republic (LO1602, LM2015086).

Acknowledgments

The authors would like to thank Prof. Malte C. Kaluza, Dr. Joachim Hein and Diethard Klöpfel from the Institute of Optics and Quantum Electronics in Jena, Germany, for supporting this work.

References

1. H. Kiriyama, A. S. Pirozhkov, M. Nishiuchi, Y. Fukuda, K. Ogura, A. Sagisaka, Y. Miyasaka, M. Mori, H. Sakaki, N. P. Dover, K. Kondo, J. K. Koga, T. Z. Esirkepov, M. Kando, and K. Kondo, "High-contrast high-intensity repetitive petawatt laser," Opt. Lett. **43**, 2595–2598 (2018).
2. D. Rostohar, J. Körner, R. Bödefeld, A. Lucianetti, and T. Mocek, "How new laser development can help laser shock peening penetration to widen industrial applications?" 2017 IEEE 3rd Int. Forum on Res. Technol. for Soc. Ind. (RTSI) **7**, 1–4 (2017).
3. J. Körner, V. Jambunathan, J. Hein, R. Seifert, M. Loeser, M. Siebold, U. Schramm, P. Sikocinski, A. Lucianetti, T. Mocek, and M. C. Kaluza, "Spectroscopic characterization of Yb^{3+}-doped laser materials at cryogenic temperatures," Appl. Phys. B **116**, 75–81 (2014).
4. D. C. Brown, "The promise of cryogenic solid-state lasers," IEEE J. Sel. Top. Quantum Electron. **11**, 587–599 (2005).
5. B. A. Reagan, C. Baumgarten, E. Jankowska, H. Chi, H. Bravo, K. Dehne, M. Pedicone, L. Yin, H. Wang, C. S. Menoni, and J. J. Rocca, "Scaling diode-pumped, high energy picosecond lasers to kilowatt average powers," High Power Laser Sci. Eng. **6** (2018).
6. M. Divoky, S. Tokita, S. Hwang, T. Kawashima, H. Kan, A. Lucianetti, T. Mocek, and J. Kawanaka, "1-J operation of monolithic composite ceramics with Yb:YAG thin layers: multi-tram at 10-Hz repetition rate and prospects for 100-Hz operation." Opt. Lett. **40**, 855–858 (2015).
7. J. Körner, J. Hein, M. Kahle, H. Liebetrau, M. Lenski, S. Pastrik, R. Seifert, and M. Kaluza, "High efficiency nanosecond pulse amplification based on diode-pumped cryogenic-cooled Yb:YAG," Adv. Opt. Mater. p. ATuE2 (2011).
8. P. Mason, M. Divoký, K. Ertel, J. Pilar, T. Butcher, M. Hanuš, S. Banerjee, J. Phillips, J. Smith, M. De Vido, A. Lucianetti, C. Hernandez-Gomez, C. Edwards, T. Mocek, and J. Collier, "Kilowatt average power 100 J-level diode pumped solid state laser," Optica **4**, 438–439 (2017).

Optics EXPRESS

9. S. De Silvestri, V. Magni, S. Taccheo, and G. Valentini, “Q-switched Nd:YAG laser with super-gaussian resonators,” Opt. Lett. **16**, 642–644 (1991).
10. M. Morin, “Graded reflectivity mirror unstable laser resonators,” Opt. Quantum Electron. **29**, 819–866 (1997).
11. A. Siegman, “Unstable optical resonators for laser applications,” Proc. IEEE **53**, 277–287 (1965).
12. S. de Silvestri, P. Laporta, V. Magni, O. Svelto, and B. Majocchi, “Unstable laser resonators with super-gaussian mirrors,” Opt. Lett. **13**, 201–203 (1988).
13. D. S. Sumida and T. Y. Fan, “Emission spectra and fluorescence lifetime measurements of Yb:YAG as a function of temperature,” Adv. Solid State Lasers p. YL4 (2004).
14. S. Banerjee, K. Ertel, P. D. Mason, P. J. Phillips, M. Siebold, M. Loeser, C. Hernandez-Gomez, and J. L. Collier, “High-efficiency 10 J diode pumped cryogenic gas cooled Yb:YAG multislab amplifier,” Opt. Lett. **37**, 2175–2177 (2012).